

Thermodynamic characterization of the stability and the melting behavior of a DNA triplex: A spectroscopic and calorimetric study

(triple helix/Hoogsteen hydrogen bonds/base triplet stability/triplex hybridization conditions/DNA recognition)

G. ERIC PLUM*, YOUNG-WHAN PARK*, SCOTT F. SINGLETON†, PETER B. DERVAN†, AND KENNETH J. BRESLAUER*‡

*Department of Chemistry, Rutgers, The State University of New Jersey, New Brunswick, NJ 08903; and †Department of Chemistry, California Institute of Technology, Mail Code 164-30, Pasadena, CA 91125

Contributed by Peter B. Dervan, September 12, 1990

ABSTRACT We report a complete thermodynamic characterization of the stability and the melting behavior of an oligomeric DNA triplex. The triplex chosen for study forms by way of major-groove Hoogsteen association of an all-pyrimidine 15-mer single strand (termed y15) with a Watson–Crick 21-mer duplex composed of one purine-rich strand (termed u21) and one pyrimidine-rich strand (termed y21). We find that the near-UV CD spectrum of the triplex can be duplicated by the addition of the B-like CD spectrum of the isolated 21-mer duplex and the CD spectrum of the 15-mer single strand. Spectroscopic and calorimetric measurements show that the triplex (y15·u21·y21) melts by two well-resolved sequential transitions. The first transition (melting temperature, T_m , $\approx 30^\circ\text{C}$) is pH-dependent and involves the thermal expulsion of the 15-mer strand to form the free duplex u21·y21 and the free single strand y15. The second transition ($T_m \approx 65^\circ\text{C}$) is pH-independent between pH 6 and 7 and reflects the thermal disruption of the u21·y21 Watson–Crick duplex to form the component single strands. The thermal stability of the y15·u21·y21 triplex increases with increasing Na^+ concentration but is nearly independent of DNA strand concentration. Differential scanning calorimetric measurements at pH 6.5 show the triplex to be enthalpically stabilized by only 2.0 ± 0.1 kcal/mol of base triplets (1 cal = 4.184 J), whereas the duplex is stabilized by 6.3 ± 0.3 kcal/mol of base pairs. From the calorimetric data, we calculate that at 25°C the y15·u21·y21 triplex is stabilized by a free energy of only 1.3 ± 0.1 kcal/mol relative to its component u21·y21 duplex and y15 single strand, whereas the 21-mer duplex is stabilized by a free energy of 17.2 ± 1.2 kcal/mol relative to its component single strands. The y15 single strand modified by methylation of cytosine at the C-5 position forms a triplex with the u21·y21 duplex, which exhibits enhanced thermal stability. The spectroscopic and calorimetric data reported here provide a quantitative measure of the influence of salt, temperature, pH, strand concentration, and base modification on the stability and the melting behavior of a DNA triplex. Such information should prove useful in designing third-strand oligonucleotides and in defining solution conditions for the effective use of triplex structure formation as a tool for modulating biochemical events.

More than three decades have passed since the first description of polynucleotide triple helices (1). In the ensuing years a small number of investigators interested in the fundamental properties of nucleic acids have studied the structure (2) and physical properties (3–6) of triple-helical nucleic acids. Most of the work in this area has focused on triple helices composed of one polypurine strand and two polypyrimidine strands; however, triplexes of (polypurine)₂·polypyrimidine also are known (7–10).

The widely accepted structural model for polypurine·(polypyrimidine)₂ triple helices is based on x-ray fiber diffraction studies on poly(A)·poly(U)₂ (2, 11) and poly(dA)·poly(dT)₂ (2, 12). In this structure, an A-form polypurine·polypyrimidine duplex joined by Watson–Crick base pairs binds the second polypyrimidine strand in its major groove. This second polypyrimidine strand interacts with the Watson–Crick duplex by means of Hoogsteen base pairing to form the base triplets TAT and C⁺GC (Fig. 1A). The formation of a triple helix from cytosine-containing third strands has been shown to be pH dependent, suggesting that the C⁺GC triplet requires protonation of the cytosine (13–15). Oligonucleotide-directed site-specific cleavage of double-helical DNA establishes that the third strand lies in the major groove parallel to the purine strand of the Watson–Crick duplex (14). Recent NMR studies on oligomeric DNA triplexes corroborate some of the structural details ascertained by less-direct techniques and provide a more detailed picture of the DNA triple helix (16–19). Additional studies are required before a complete picture of triplex structures and their sequence dependence emerges.

Recent interest in triple helical DNA has been stimulated by the discovery of triplex-containing structures, such as H-form DNA, which have been proposed to explain the enhanced sensitivity of mirror repeat polypurine·polypyrimidine sequences to chemical modification (20–22). Moreover, oligonucleotide-directed triple helix formation has the potential to be a general solution for DNA recognition, which has implications for physical mapping of chromosomes and site-specific inhibition of transcription *in vivo* (14, 15, 23–28).

A prerequisite for predicting the relative affinities of target duplex domains toward third-strand hybridization is thermodynamic data on the temperature and sequence-dependent stabilities of DNA triplex structures as a function of solution conditions. Although a few such studies for an RNA triplex exist (29–31), the relevant thermodynamic data for DNA triplexes are nonexistent. To determine the thermodynamics of a DNA triplex, three oligodeoxyribonucleotides were synthesized: a pyrimidine 15-mer sequence, designated y15, and two complementary 21-mer sequences, u21 and y21, where the “y” prefix indicates a pyrimidine-rich strand and the “u” prefix designates a purine-rich strand (Fig. 1B). We selected these sequences, in part, because the strand orientation within the y15·u21·y21 triplex is well characterized (14, 15). From mixing curves we demonstrate that, under appropriate conditions, the three strands combine to form a triplex containing one strand of each oligodeoxyribonucleotide. Temperature-dependent UV absorbance spectroscopy and differential scanning calorimetry (DSC) were used to determine the stability and the melting behavior of the oligomeric

The publication costs of this article were defrayed in part by page charge payment. This article must therefore be hereby marked “advertisement” in accordance with 18 U.S.C. §1734 solely to indicate this fact.

Abbreviations: T_m , melting temperature; DSC, differential scanning calorimetry.

‡To whom reprint requests should be addressed.

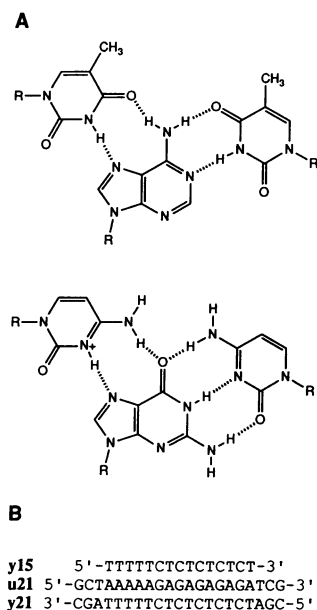


FIG. 1. (A) Nucleotide base triplets: T·A·T and C⁺·G·C. (B) Sequences of the three oligonucleotides along with their designations. The sequences are displayed to emphasize the complementarity and polarity of the strands in the triplex.

DNA triplex as a function of solution conditions, thereby providing a complete thermodynamic characterization of a DNA triple-helical structure.

MATERIALS AND METHODS

Oligodeoxyribonucleotide Synthesis and Purification. Molecules were synthesized using standard solid-phase cyanophosphoramidite methods (32). Purification of all the sequences was accomplished by HPLC (33), whereas gel electrophoresis also was used for purification of the one modified sequence. HPLC analysis of the enzyme degradation products of the oligomers revealed that each sequence exhibited the expected ratios of nucleosides.

The extinction coefficient (ϵ) for each oligomer was determined by phosphate analysis (34) yielding the following values at 260 nm and 25°C: $1.166 \times 10^5 \text{ M}^{-1}\text{cm}^{-1}$ for y15; $1.846 \times 10^5 \text{ M}^{-1}\text{cm}^{-1}$ for u21; and $1.965 \times 10^5 \text{ M}^{-1}\text{cm}^{-1}$ for y21. All concentrations, unless otherwise noted, are designated on a per strand basis and were determined spectrophotometrically using the experimentally measured ϵ values.

Buffers. Unless otherwise indicated, all measurements were conducted in 10 mM sodium phosphate containing 0.1 mM EDTA and 200 mM NaCl, at pH 6.5. The final pH was adjusted to the desired value using 0.1 M HCl or 0.1 M NaOH.

UV Mixing Curves. Stock solutions of the u21 and the y21 single strands were prepared at equal concentrations (2.5 μM). To construct a u21·y21 duplex mixing curve, 100 μl of either the y21 or u21 solution was added to a 1-cm pathlength cuvette containing 600 μl of the stock solution of the complementary 21-mer strand. After each addition, the cuvette was inverted repeatedly to ensure complete mixing followed by equilibration at 15°C for 20 min. After equilibration, the absorbance at 260 nm was measured. Construction of a triplex mixing curve was accomplished similarly. In this case, the two solutions used were the previously constituted u21·y21 duplex (2.5 μM duplex) and a solution of the y15 single strand (2.5 μM strand).

UV Spectroscopy. Absorbance versus temperature profiles were obtained at 260 nm at a heating rate of 0.5°C/min using a computer-interfaced Perkin-Elmer model 575 spectropho-

tometer equipped with a thermoelectrically controlled cell holder. The melting temperature (T_m) for each transition was obtained from the optical melting curves by using previously described protocols (35–38). Melting temperatures were determined over a range of oligomer concentrations (1.6–50 μM), sodium ion concentrations (0.02–1.0 M), and pH (pH 6 to 7).

CD Spectroscopy. CD spectra from 320 to 220 nm were recorded on an AVIV model 60DS spectropolarimeter (Aviv Associates, Lakewood, NJ) equipped with a thermoelectrically controlled cell holder using the same samples employed in the UV melting studies. Each spectrum reported is an average of at least three scans.

Differential Scanning Calorimetry. Apparent excess heat capacity (ΔC_p) versus temperature (T) profiles for the order–disorder transitions of the duplex and the triplex were obtained by using a MC-2 differential scanning calorimeter (Microcal, Amherst, MA). The ΔC_p was recorded continuously while the temperature was increased from 7°C to 100°C at a rate of 60°C/hr. The triplex concentration in the DSC experiments was 58 μM . The transition enthalpy (ΔH^0) was calculated from the area under the calorimetric ΔC_p versus T curve ($\Delta H^0 = \int \Delta C_p dT$). The transition entropy (ΔS^0) was calculated by integrating the area under the corresponding $\Delta C_p/T$ versus T curve [$\Delta S^0 = \int (\Delta C_p/T) dT$].

RESULTS AND DISCUSSION

Stoichiometry of the Complexes. The stoichiometry of each complex was established by the method of continuous fractions (39, 40). Fig. 2 shows the mixing curve for the two 21-mer sequences, u21 and y21. The inflection point at 0.5 mole fraction establishes the formation of the expected 1:1 complex for the duplex. An ϵ of $3.15 \times 10^5 \text{ M}^{-1}\text{cm}^{-1}$ can be estimated for the duplex from the absorbance at the inflection point.

The stoichiometry for the complex formed by addition of the y15 sequence to the duplex formed by the two 21-mer sequences u21 and y21 can be obtained in a similar fashion. As shown in Fig. 2, an inflection point at a mole fraction of 0.5 is observed. Therefore, the combination of the two 21-mer strands and the 15-mer strand results in the formation of a triplex. From the absorbance at the inflection point, ϵ for the triplex can be estimated to be $4.14 \times 10^5 \text{ M}^{-1}\text{cm}^{-1}$.

These mixing experiments establish that the three sequences chosen for study (u21, y21, and y15) can be added together stoichiometrically to form either a Watson–Crick duplex (u21·y21) or a Hoogsteen–Watson–Crick triplex (y15·u21·y21). This knowledge provides us with a framework for conducting the physical studies described below.

The Triplex Melts in Two Steps: Loss of the y15 Third Strand Followed by Disruption of the Released 21-mer Duplex. We monitored the thermally induced disruption of the triplex by measuring the temperature-dependent absorbance change at

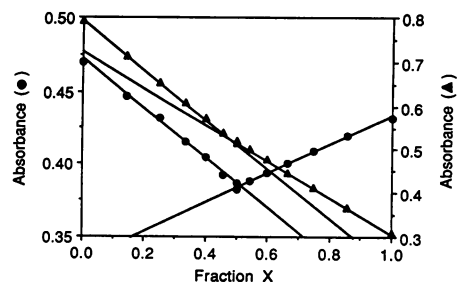


FIG. 2. UV mixing curves for formation of complexes. (●) Mixing of the u21 single strand with the y21 single strand to form the u21·y21 duplex. Values on the abscissa are mole fraction of y21. (▲) Mixing of the u21·y21 duplex with the y15 single strand to form the y15·u21·y21 triplex. Values on the abscissa are mole fraction of y15.

260 nm, as shown in Fig. 3, trace A. Note that the triplex melts in two sequential well-resolved steps. We assign the high-temperature transition to the melting of the 21-mer duplex and the low-temperature transition to the thermally induced release of the y15 strand from the triplex to form the 21-mer duplex and the free y15 single strand. These assignments are supported by the observations described below.

We measured the UV melting profile for the thermally induced disruption of the isolated 21-mer duplex. This melting curve is shown in Fig. 3, trace B. A comparison between Fig. 3, traces A and B, reveals that under comparable conditions the melting transition of the free duplex coincides exactly with the high-temperature melting transition of the triplex. This observation supports our conclusion that the second transition in Fig. 3, trace A, corresponds to duplex disruption.

Our studies of the pH dependence of the two melting transitions further assist us in defining the events associated with each transition. Fig. 4 shows the pH dependence for the T_m of each transition. The upper line in this figure shows that the high-temperature transition is independent of pH between pH 6 and 7. This pH-independent melting behavior is consistent with the known pK_a values of the bases in a Watson-Crick DNA duplex and further supports our assignment of the second transition to the melting of the u21-y21 duplex. By contrast, the lower line in Fig. 4 reveals that the T_m of the low-temperature transition exhibits a clear pH dependence. This observation is consistent with at least partial protonation of the cytosines on the third strand, thereby supporting our assignment of the first transition to triplex expulsion of the y15 single strand. Thus, the pH dependence of T_m supports our assignments of the molecular events associated with each transition.

Dependence of Triplex Formation and T_m on Salt Concentration. To define optimal hybridization conditions for triplex formation, it is necessary to evaluate the influence of salt concentration on triplex thermal stability. We find that a Na^+ concentration of 200 mM is sufficient to induce complete y15-u21-y21 triplex formation, even in the absence of Mg^{2+} . Below 200 mM Na^+ , triplex formation is incomplete, as judged by a reduction in hyperchromicity of the first melting transition. To be specific, at 24 mM Na^+ no triplex forms. At 111 mM Na^+ , approximately two-thirds of the triplex forms. At Na^+ concentrations above 200 mM, the apparent hyperchromicity of the first transition is constant, thereby suggesting complete formation of the triplex. By contrast, over this same range of salt concentrations (0.024–1 M), the hyperchromicity of the second transition is independent of Na^+ concentration, thereby suggesting that the 21-mer duplex is fully formed over this entire range of solution conditions. Thus, for this system, changes in the Na^+ concentration between 24 and 200 mM can be used to modulate the degree of triplex formation without disrupting the target host duplex.

For Na^+ concentrations where the triplex is fully formed (0.2–1 M), we find the T_m of the first triplex transition (y15-u21-y21 \rightleftharpoons u21-y21 + y15) to be linearly dependent on

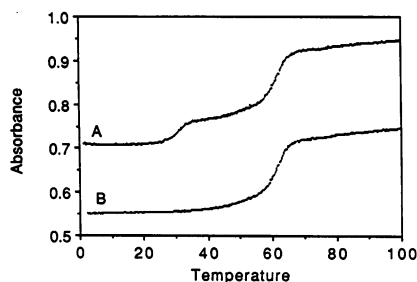


FIG. 3. UV absorbance versus temperature profiles of complexes. Traces: A, y15-u21-y21 triplex; B, u21-y21 duplex.

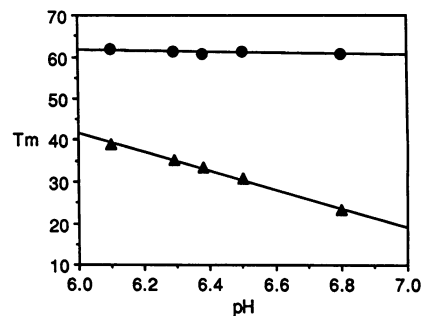


FIG. 4. Effects of pH on T_m . (▲) Triplex disruption (y15-u21-y21 \rightleftharpoons u21-y21 + y15). (●) Duplex disruption (u21-y21 + y15 \rightleftharpoons u21 + y21 + y15).

$\log[Na^+]$, with $\partial T_m / \partial \log[Na^+] = 12.1$. This derivative provides a quantitative measure of how much one can thermally stabilize the triplex by increasing the Na^+ concentration.

The Triplex CD Spectrum Is Reproduced by the Sum of the Component Duplex and Single-Strand Spectra. CD spectra between 220 and 320 nm were measured for the duplex, the triplex, and their component single strands. The spectrum for the 21-mer duplex (u21-y21) is composed of two bands of comparable intensity and is consistent with a B-like double helix (35, 41). At 20°C, a negative band with maximum intensity at 247 nm and a positive band with maximum intensity at 280 nm are observed. When the temperature is increased to 45°C, the positive band shifts to 276 nm and grows in intensity while the negative band declines slightly in intensity and shifts to about 246 nm. At 80°C, the positive band shifts to 273 nm and decreases in intensity while the negative band intensity decreases precipitously. This temperature-dependent behavior is consistent with the expected CD melting properties of a B-form DNA duplex (41).

The CD spectrum observed for the triplex can be duplicated by the sum of the CD spectrum of the y15 single strand and the CD spectrum of the isolated duplex. At 80°C, the CD spectrum is reproduced by the sum of the individual strand spectra at 80°C. At 20°C, which is below the first transition, and at 45°C, which is between the two transitions, the sum of the duplex CD spectrum and the y15 CD spectrum satisfactorily reproduces the CD spectrum we measure for the triplex. This additivity is both interesting and surprising since recent NMR studies on oligonucleotides (17, 18) suggest that some or all of the strands adopt an A-DNA-like conformation upon triplex formation. Perhaps fortuitous compensation masked CD changes for this system. Alternatively, the final conformation of a triplex may prove to be sequence dependent. Unfortunately, from the available x-ray fiber diffraction and NMR data, it is not yet possible to evaluate the dependence of triplex structure on sequence. However, our measurements demonstrate that triplex formation is not necessarily accompanied by a change in the near-UV CD relative to its component duplex and single strand.

The Triplex Is Thermodynamically Much Less Stable Than Its Host Duplex. The utility of DNA triplex formation as a method to modulate a range of biological activities will, in large part, depend on the ability to assess if a given oligonucleotide will form selectively a stable triplex structure under specific hybridization conditions. Such an assessment requires thermodynamic data on triplex structures as a function of base sequence, chain length, salt, pH, and temperature. We have used DSC to obtain directly some of the requisite thermodynamic data for the DNA triplex studied in this work.

The calorimetric heat capacity versus temperature profiles for the triplex and the isolated duplex are shown in Fig. 5. Inspection of these figures reveals that the triplex melts by two well-resolved transitions (Fig. 5, trace A), whereas the

isolated duplex melts by a single transition (Fig. 5, trace B). Both of these melting behaviors are fully consistent with the optical melting profiles (see Fig. 3). The T_m values of each DSC transition agree exactly with those derived from the optical measurements under comparable conditions. Repeated heating and cooling of the DSC samples produced superimposable thermograms, thereby demonstrating the reversibility of the equilibria associated with triplex formation. We also found that changing the heating rate does not alter the thermodynamic parameters, thereby demonstrating that the equilibria under study are not kinetically limited.

Calorimetric transition enthalpies were calculated by integrating the area under each heat capacity versus temperature curve. These data are summarized in Table 1. Inspection of these enthalpy data reveals a number of interesting features. First, the enthalpy change associated with the second transition of the triplex (128 kcal/mol) is in excellent agreement with the enthalpy change for disruption of the isolated duplex (133 kcal/mol), which in turn is in good agreement with the predicted enthalpy change of 143 kcal/mol calculated from a nearest-neighbor analysis (42). van't Hoff enthalpies derived from optical melting curves and DSC shape analysis (37) also are in good agreement with the calorimetric enthalpy. These agreements in the enthalpy data provide additional confirmation of our assignment of the second transition to duplex disruption. Further inspection of the data in Table 1 reveals that the transition enthalpy per base interaction for triplex dissociation is much lower than for duplex dissociation. Specifically, at pH 6.5, we measure 2.0 ± 0.1 kcal/mol of base triplets for the transition from triplex to duplex plus single strand and 6.3 ± 0.3 kcal/mol of base pairs for the transition from duplex to single strand. It is interesting to note that the triplex transition enthalpy data we measure is similar to the value that has been measured for a polymeric RNA triplex (30, 31). Specifically, Krakauer and Sturtevant (30) report an enthalpy of about 1.3 kcal/mol of base triplets for the dissociation of poly(A)-poly(U)₂ to poly(A)-poly(U) + poly(U). Thus, for the polymeric RNA triplex and the oligomeric DNA triplex calorimetrically studied to date, the third-strand dissociation enthalpies are small and positive. By contrast, van't Hoff enthalpies derived from optical melting curves and DSC shape analysis (37) are about 3 times the calorimetric enthalpy. This disparity suggests that caution should be exercised when attempting to extract thermodynamic data for triplexes from optical studies (43).

The entropic contribution to the triplex and to the duplex transitions may be calculated from the area under the secondary $\Delta C_p/T$ versus T curves, which can be derived from the experimental ΔC_p versus T profiles (37). These data also are reported in Table 1. Inspection of these data reveals the expected large and positive entropy changes favoring structure disruption. Note, however, that the entropy contributes less to triplex than to duplex disruption, as one might

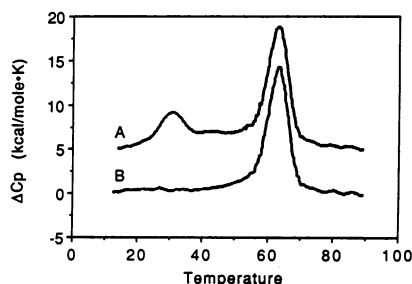


FIG. 5. Calorimetric apparent ΔC_p versus temperature profiles. Traces: A, y15-u21-y21 triplex; B, isolated u21-y21 duplex. For the sake of clarity, trace A is displaced by 5 kcal/mol·K.

Table 1. Calorimetrically determined thermodynamic parameters for the melting transitions of the y15-u21-y21 triplex

Transition	T_m , °C	ΔH^0 , kcal/mol	ΔS^0 , cal/mol·K	ΔG^0 , kcal/mol
First triplex y15-u21-y21 → u21-y21 + y15	30.0	30.4 ± 2	97.6 ± 7	1.3 ± 0.1
Second triplex u21-y21 + y15 → u21 + y21 + y15	65.7	128 ± 8	370 ± 24	17.2 ± 1.6
Duplex u21-y21 → u21 + y21	64.7	133 ± 6	388 ± 15	17.2 ± 1.2

Triplex and duplex data represent the averages of four and three measurements, respectively. Errors shown represent ± 1 standard deviation.

anticipate considering the order that still remains in the products after the initial disruption of the triplex.

Given the enthalpic and entropic contributions we have measured calorimetrically at the T_m and assuming a negligible difference in heat capacity between the initial and final states, the free energy at any reference temperature can be calculated using the standard thermodynamic relationship $\Delta G^0 = \Delta H^0 - T\Delta S^0$. Table 1 includes the free-energy data at 25°C calculated in this manner. Inspection of these ΔG^0 data reveals that at 25°C and 200 mM Na⁺, the triplex structure is only marginally stable ($\Delta G^0 = 1.3$ kcal/mol) relative to the significant stability of its host duplex ($\Delta G^0 = 17.2$ kcal/mol). Nevertheless, this relatively small ΔG^0 of 1.3 kcal/mol corresponds to an association constant (K) of ≈ 9.0 , which means that for this system under the equilibrium conditions employed the vast majority of third strands are bound to the target duplex sequence. Interestingly, this marginal stability of the fully bonded triplex may be of practical importance since it will reduce the probability of probe hybridization to secondary duplex sites containing sequences that are similar but not fully "complementary" to a third-strand probe (e.g., mismatches). Thus, the application of high ionic strengths and low pH to enhance triplex stability may not always be desirable, since one seeks conditions that optimize, but do not necessarily maximize, third-strand binding.

The Triplex Melts as if Monomolecular. To design optimal hybridization conditions for triplex formation, it is necessary to evaluate the influence of strand concentration on triplex thermal stability. To this end, we have measured how the triplex T_m varies with total strand concentration (C_T).

Triplex formation by the association of a third strand (e.g., y15) with a host duplex (e.g., u21-y21) formally is a bimolecular process. Consequently, the position of this equilibrium and, therefore, the T_m should, in principle, depend on the C_T . Traditionally, this dependence is assessed by measuring the slope of a plot of T_m^{-1} versus $\ln C_T$ (35). Such a plot should be linear with a slope that depends on both the enthalpy of complex formation, ΔH^0 , and the molecularity (37). We have measured the dependence of T_m^{-1} on $\ln C_T$ for the triplex and find the slope to be nearly a factor of 30 less than expected based on the calorimetrically measured triplex transition enthalpy of 30.4 kcal/mol and the formal molecularity of two (37). Thus, we conclude that, for the sequences studied here, triplex formation is approaching the limit of pseudo-first-order behavior, as is observed for association/dissociation equilibria in polymeric DNA systems. This limiting behavior occurs when the monomolecular triplex elongation ("growth") steps dominate the bimolecular nucleation ("initiation") steps (35). In such cases, even an equilibrium with a formal molecularity greater than unity will functionally behave as if it were monomolecular.

On a practical level, the results described above mean that for the triplex studied here one cannot significantly increase the thermal stability simply by using higher concentrations of the third strand and that triplex thermodynamic parameters extracted from concentration-dependent melting studies will be in error.

Methylation of the Third-Strand Cytosines Enhances the Stability of the Triplex. To examine the effects of base modification on triplex stability, we also have studied the analogue of the y15 single strand in which all cytosines are C-5-methylated [Me-y15]. This modified single strand exhibits an ϵ value of $1.069 \times 10^5 \text{ M}^{-1}\text{cm}^{-1}$ at 260 nm and 25°C. We find that triplexes also form readily when the u21-y21 duplex is mixed with the Me-y15 single strand. The mixing curves and the UV-monitored thermal melting profiles we measure for the Me-y15-containing triplex are qualitatively similar to those of the triplex produced from the unmodified third strand y15. Furthermore, the CD spectra are similar to those for the unmodified triplex, thereby suggesting that the modification does not alter the global triplex structure. As with the unmodified system, we find the transition from triplex to duplex plus single strand (Me-y15) to be nearly independent of oligomer concentration.

The pH dependence of T_m for the transition from triplex to duplex plus Me-y15 single strand is the same as that which we measured for the triplex with the unmodified single strand (y15). In other words, the slopes of the T_m versus pH curves are the same for the modified and unmodified triplex systems. Significantly, however, we find the Me-y15-containing triplex to be thermally more stable by 10°C at any given pH. For example, at pH 6.5 the y15 triplex melts at 29.9°C whereas the Me-y15 triplex melts at 40.0°C. Such enhancement of triplex stability by cytosine methylation has been observed in polymeric systems (44) and in oligonucleotide-directed site-specific binding of large duplex DNA (15).

It is of interest to compare the difference in the known pK_a values of the unmodified and modified cytosine monomers with the apparent pK_a difference we deduce from our melting measurements. The pK_a of dCMP is 4.6, whereas the pK_a of 5-methyldeoxycytosine 5'-monophosphate is 4.4, thereby reflecting a methylation-induced ΔpK_a of -0.2 unit (45). By contrast, based on the observed triplex melting behavior, we calculate an apparent methylation-induced ΔpK_a of $+0.5$ unit. This result is consistent with that obtained on essentially the same sequences using the affinity cleaving method (15). Thus, it is possible that increased hydrophobicity imparted to the third strand by methylation, rather than just a change in the cytosine pK , is responsible for part, if not all, of the enhancement of triplex stability that we observe with the modified third strand (15).

The practical consequence of this study on the modified triplex is that cytosine methylation at C-5 provides one approach for altering a third-strand oligonucleotide in a manner that increases the thermal stability of the resultant triplex (15). This approach may prove useful for modulating the biological activities controlled by triplex formation.

Concluding Remarks. The development and expanded use of oligonucleotides (or their analogues) for modulating biochemical activities through site-specific triplex formation demands an understanding of how triplex stability depends on chain length, pH, salt, base sequence, and base modifications. Compiling the requisite body of thermodynamic data is a minimum first step toward making these assessments.

K.J.B. wishes to dedicate this paper to Daniel Michael Breslauer

for teaching him the importance of adding a third strand to an already existing duplex. This work was supported by the National Institutes of Health Grants GM23509 (K.J.B.), GM34469 (K.J.B.), and GM35724 (P.B.D.).

- Felsenfeld, G., Davies, D. R. & Rich, A. (1957) *J. Am. Chem. Soc.* **79**, 2023–2024.
- Arnott, S., Bond, P. J., Selsing, E. & Smith, P. J. C. (1976) *Nucleic Acids Res.* **3**, 2459–2470.
- Stevens, C. L. & Felsenfeld, G. (1964) *Biopolymers* **2**, 293–314.
- Riley, M., Maling, B. & Chamberlin, M. J. (1966) *J. Mol. Biol.* **20**, 369–389.
- Blake, R. D., Massoulié, J. & Fresco, J. R. (1967) *J. Mol. Biol.* **30**, 291–308.
- Morgan, A. R. & Wells, R. D. (1968) *J. Mol. Biol.* **37**, 63–80.
- Lipsett, M. (1964) *J. Biol. Chem.* **239**, 1256–1260.
- Inman, R. B. (1964) *J. Mol. Biol.* **10**, 137–146.
- Broitman, S. L., Im, D. D. & Fresco, J. R. (1987) *Proc. Natl. Acad. Sci. USA* **84**, 5120–5124.
- Letai, A. G., Pallidino, M. A., Fromm, E., Rizzo, V. & Fresco, J. R. (1988) *Biochemistry* **27**, 9108–9112.
- Arnott, S. & Bond, P. J. (1973) *Nature (London) New Biol.* **244**, 99–101.
- Arnott, S. & Selsing, E. (1974) *J. Mol. Biol.* **88**, 509–521.
- Lee, J. S., Johnson, D. A. & Morgan, A. R. (1979) *Nucleic Acids Res.* **6**, 3073–3091.
- Moser, H. E. & Dervan, P. B. (1987) *Science* **238**, 645–650.
- Povsic, T. J. & Dervan, P. B. (1989) *J. Am. Chem. Soc.* **111**, 3059–3061.
- Rajagopal, P. & Feigon, J. (1989) *Nature (London)* **339**, 637–640.
- Rajagopal, P. & Feigon, J. (1989) *Biochemistry* **28**, 7859–7870.
- de los Santos, C., Rosen, M. & Patel, D. (1989) *Biochemistry* **28**, 7282–7289.
- Pilch, D. S., Levenson, C. & Shafer, R. H. (1990) *Proc. Natl. Acad. Sci. USA* **87**, 1942–1946.
- Mirkin, S. M., Lyamichev, V. I., Drushlyak, K. N., Dobrynin, V. N., Filippov, S. A. & Frank-Kamenetskii, M. D. (1987) *Nature (London)* **330**, 495–497.
- Wells, R. D., Collier, D. A., Hanvey, J. C., Shimizu, M. & Wohlrab, F. (1988) *FASEB J.* **2**, 2939–2949.
- Htun, H. & Dahlberg, J. E. (1989) *Science* **243**, 1571–1576.
- Strobel, S. A., Moser, H. E. & Dervan, P. B. (1988) *J. Am. Chem. Soc.* **110**, 7927–7929.
- François, J.-C., Saison-Behmoaras, T., Barbier, C., Chassignol, M., Thoung, N. T. & Hélène, C. (1989) *Proc. Natl. Acad. Sci. USA* **86**, 9702–9706.
- Prasenth, D., Perroualt, L., Doan, T. L., Chassignol, M., Thoung, N. & Hélène, C. (1988) *Proc. Natl. Acad. Sci. USA* **85**, 1349–1353.
- Sun, J.-S., François, J.-C., Montenay-Garestier, T., Saison-Behmoaras, T., Roig, V., Thoung, N. T. & Hélène, C. (1989) *Proc. Natl. Acad. Sci. USA* **86**, 9198–9202.
- Maher, L. J., III, Wold, B. & Dervan, P. B. (1989) *Science* **245**, 725–730.
- Hanvey, J. C., Shimizu, M. & Wells, R. D. (1990) *Nucleic Acids Res.* **18**, 157–161.
- Ross, P. D. & Scruggs, R. L. (1965) *Biopolymers* **3**, 491–496.
- Krakauer, H. & Sturtevant, J. M. (1968) *Biopolymers* **6**, 491–512.
- Neumann, E. & Ackermann, T. (1969) *J. Phys. Chem.* **73**, 2170–2178.
- Sinha, N. D., Biernat, J. & Köster, M. (1983) *Tetrahedron Lett.* **24**, 5843–5846.
- Gaffney, B. L. & Jones, R. A. (1989) *Biochemistry* **28**, 5881–5889.
- Snell, F. D. & Snell, C. T. (1949) *Colorimetric Methods of Analysis* (Van Nostrand, New York), 3rd Ed., Vol. 2, p. 671.
- Cantor, C. R. & Schimmel, P. R. (1980) *Biophysical Chemistry* (Freeman, San Francisco).
- Breslauer, K. J. (1986) in *Thermodynamic Data for Biochemistry and Biotechnology*, ed. Hinz, H. J. (Springer, New York), pp. 402–427.
- Marky, L. A. & Breslauer, K. J. (1987) *Biopolymers* **26**, 1601–1620.
- Gralla, J. & Crothers, D. M. (1973) *J. Mol. Biol.* **73**, 497–511.
- Job, P. (1928) *Ann. Chim. (Paris)* **9**, 113–134.
- Felsenfeld, G. & Rich, A. (1957) *Biochim. Biophys. Acta* **26**, 457–468.
- Bush, C. A. (1974) in *Basic Principles in Nucleic Acid Chemistry*, ed. T'so, P. O. P. (Academic, New York), Vol. 2, pp. 91–169.
- Breslauer, K. J., Frank, R., Blöcker, H. & Marky, L. A. (1986) *Proc. Natl. Acad. Sci. USA* **83**, 3746–3750.
- Manzini, G., Xodo, L. E., Gasparotto, D., Quadrioglio, F., van der Marel, G. A. & van Boom, J. H. (1990) *J. Mol. Biol.* **213**, 833–843.
- Lee, J. S., Woodsworth, M. L., Latimer, L. J. P. & Morgan, A. R. (1984) *Nucleic Acids Res.* **12**, 6603–6614.
- Dunn, D. B. & Hall, R. H. (1975) in *Handbook of Biochemistry and Molecular Biology*, ed. Fasman, G. P. (CRC, Cleveland, OH), 3rd Ed., Vol. 1, pp. 198–199.